

NEURAL NETWORK-BASED ACOUSTIC VEHICLE COUNTING

Slobodan Djukanović¹

Yash Patel¹

Jiří Matas¹

Tuomas Virtanen²

¹ Czech Technical University, Faculty of Electrical Engineering, Prague, Czech Republic

²Tampere University, Audio Research Group, Tampere, Finland

ABSTRACT

This paper addresses acoustic vehicle counting using one-channel audio. We predict the pass-by instants of vehicles from local minima of a vehicle-to-microphone distance predicted from audio. The distance is predicted via a two-stage (coarse-fine) regression, both realised using neural networks (NNs). Experiments show that the NN-based distance regression outperforms by far the previously proposed support vector regression. The 95% confidence interval for the mean of vehicle counting error is within $[0.28\%, -0.55\%]$. Besides the minima-based counting, we propose a deep learning counting which operates on the predicted distance without detecting local minima. Results also show that removing low frequencies in features improves the counting performance.

Index Terms— Vehicle counting, log-mel spectrogram, neural network, peak detection, deep learning.

1. INTRODUCTION

Traffic monitoring (TM) systems use different traffic data to improve the use and performance of roadway systems, transportation safety, law enforcement, prediction of future transportation needs etc. TM data include estimates of vehicle count, traffic volume, speed of vehicles and of various vehicle parameters (length, weight, class) [1].

Current TM systems use diverse sensors and technologies, including induction loops, vibration, piezoelectric, infrared, ultrasonic, magnetic and acoustic sensors and cameras [1]. Vision-based TM systems have recently become popular due to breakthroughs in object detection, tracking and classification tasks provided by deep learning methods [2]. In addition, a single camera suffices to cover multiple lanes for the TM tasks, which is not the case for other sensor technologies. However, in addition to high computational complexity, issues like partial occlusion, shadows and illumination variation limit the performance of vision-based TM systems [1, 3].

Acoustic TM has several advantages in comparison with the vision-based one [1]. Microphones are less expensive than

cameras, consume less energy, require less storage space, are easier to install and maintain with low wear and tear. In addition, acoustic TM is not affected by visual occlusions and lighting conditions, and has less privacy issues.

This paper addresses acoustic vehicle counting using one-channel audio. The standard approach is to detect temporal variation of the sound power due to vehicles passing by the acoustic sensor [4–6], which is performed using state transitions of a hidden Markov model [4] or by a peak-picking algorithm [5, 6]. Maximal frequency at which the power of a time-frequency representation reaches a predefined threshold, a.k.a. top-right frequency, also enables detecting vehicles passing by the microphone [7]. The method [8] uses a prediction of a pseudo-distance between a vehicle and the microphone referred to as *clipped vehicle-to-microphone distance*. Vehicle counting [8], carried out by counting local minima in the predicted distance, outperforms those based on peak detection in the sound power and top-right frequency. However, the optimal, false negative - false positive compensating, detection threshold in [8] can only be imprecisely estimated *a priori*. Moreover, the distance regression [8] is computationally demanding.

In this paper, we significantly improve the distance regression, and thus counting accuracy, compared to [8] by a computationally less demanding approach. We first overview clipped vehicle-to-microphone distance (Section 2) and then propose new counting method (Section 3). Experimental results are given in Section 4 and Section 5 concludes the paper.

2. CLIPPED VEHICLE-TO-MICROPHONE DISTANCE AND VEHICLE COUNTING

In [8], clipped vehicle-to-microphone distance¹ of the k -th vehicle is defined as

$$d^{(k)}(t) = \begin{cases} |t - T^{(k)}|, & |t - T^{(k)}| < T_d \\ T_d, & \text{elsewhere,} \end{cases} \quad (1)$$

where $T^{(k)}$ represents the pass-by instant and T_d is the distance threshold. The V-shape of $d^{(k)}(t)$ models approaching and receding of the vehicle from the microphone (see dotted

The research was supported by Research Center for Informatics (project CZ.02.1.01/0.0/0.0/16019/0000765 funded by OP VVV) and CTU student grant (SGS OHK3-019/20). Slobodan Djukanović was supported by the OP RDE programme of project International Mobility of Researchers MSCA-IF III at CTU in Prague No. CZ.02.2.69/0.0/0.0/19_074/0016255.

¹We will refer to clipped vehicle-to-microphone distance as the distance.

line around $T^{(1)}$ in Fig. 1). When the audio contains N_v vehicles, only the distance of the closest vehicle is taken into account, so the overall distance is defined as minimum of all separate distances (dotted line in Fig. 1):

$$D(t) = \min\{d^{(1)}(t), d^{(2)}(t), \dots, d^{(N_v)}(t)\}. \quad (2)$$

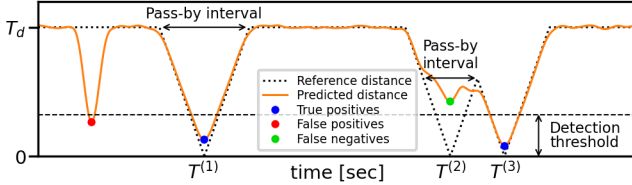


Fig. 1. Illustration of a reference distance, distance predicted from audio and classification of predicted distance minima.

In [8], the vehicle count is equal to the number of detected local minima of the predicted distance (orange line in Fig. 1) that fall below a detection threshold. Not every local minimum below the threshold corresponds to a vehicle passing by the microphone. Only minima that occur within the true vehicle pass-by intervals (horizontal arrows in Fig. 1) represent true positives (TPs). Other minima below the threshold represent false positives (FPs), whereas minima that occur within the corresponding pass-by intervals, but are above the threshold, represent false negatives (FNs).

The method [8] is evaluated using the TP, FP and FN probabilities, p_{TP} , p_{FP} and p_{FN} , calculated for variable detection threshold. The optimal threshold is obtained at point where $p_{FP} = p_{FN}$, since then the FPs and the FNs cancel each other in statistical sense and the total number of detected vehicles equals the true number of vehicles. In terms of counting error, the best generalization in [8] is obtained when the distance is predicted using the log-mel spectrogram (LMS) and newly introduced high-frequency power (HFP) as input features. With HFP, the counting error remains low (below 2%) within a wide range of detection threshold values.

Although characterized by a low counting error within a wide range of detection thresholds, the optimal threshold of [8] is not known in advance. Our first objective is to extend the low-error threshold range (below 2% or even more), i.e., to make counting more robust to the choice of detection threshold. Another drawback of [8] is the computational complexity. For distance regression, it uses support vector regression (SVR), implemented in the libsvm library [9]. Its complexity scales between $O(n_f n_s^2)$ and $O(n_f n_s^3)$, where n_f and n_s represent the number of features and samples in the dataset, respectively. Therefore, our second objective is to perform distance regression in a computationally more efficient way to enable scaling to larger datasets. A method which fulfills these two objectives is described in the sequel.

3. NEURAL NETWORK-BASED COUNTING

To address the low-counting error objective, we propose to improve the accuracy of distance regression. To that end, we carry out a two-stage (coarse-fine) regression. To address the computational complexity objective, we propose to use fully-connected neural networks (FCNNs) instead of originally used SVR. The block diagram of the proposed method is presented in Fig. 2 (top). $x_i(t_0)$, $i = 1, \dots, M$ are input features at time instant t_0 and $\hat{D}(t_0)$ represents the predicted distance at t_0 . The *Vehicle counting* block carries out counting based on the distance prediction of the whole audio file.

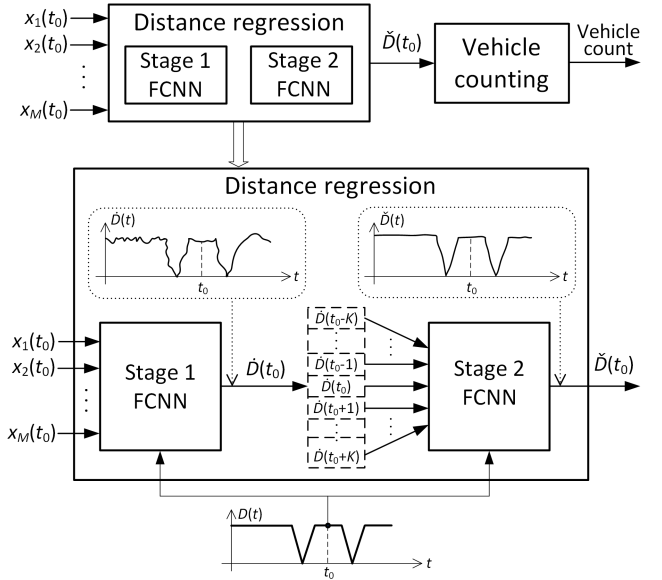


Fig. 2. Top: The block diagram of the proposed vehicle counting method. Bottom: Distance regression in detail. Stage 2 improves the distance regression output by Stage 1.

3.1. Distance regression and input features

A detailed representation of the proposed distance regression is given in Fig. 2 (bottom). Stage 1 FCNN performs regression based on input features, similarly to SVR in [8]. A vector of $2K + 1$ successive distances $\hat{D}(t_0 - K), \dots, \hat{D}(t_0 + K)$ predicted by Stage 1 FCNN, centered at t_0 , represents input features to Stage 2 FCNN. The task of Stage 2 FCNN is to refine the output of Stage 1.

As input features, we use the HFP+LMS combination, as suggested in [8]. Since HFP represents the power of high-frequency portion of the signal spectrum, we incorporate it into LMS by leaving out a number of filters with the lowest central frequencies in the mel spectrogram filter bank [10]. The resulting LMS, referred to as high-frequency LMS (HF-LMS), does not include low-frequency portion of the spectrum which contains the most significant part of the environ-

ment noise. To take into account time dependence between adjacent $D(t)$ values, the value $D(t_0)$ will be predicted using the samples of the HF-LMS spectrum at instant t_0 and Q preceding and following instants (for details, see Section 3.3).

Prior to vehicle counting, the predicted distance is low-pass filtered to eliminate high-frequency oscillations, which is discussed in Section 4.

3.2. Vehicle counting

In this paper, we propose two vehicle counting approaches, both based on the final (Stage 2) predicted distance.

3.2.1. Peak properties-based vehicle counting

In [8], local minima of the predicted distance were detected by detecting peaks (local maxima) of the inverted distance (see dashed line in Fig. 3 (bottom)) based on their prominence². Here, we extend this approach by introducing a peak magnitude criterion. If two close peaks have similar magnitudes (corresponding to two close vehicles), the prominence of the weaker one can be much less than that of the stronger one. The weaker peak can be left out if it is detected based on prominence only. Therefore, we define vehicle detection as:

A vehicle is detected if detected peak of the inverted predicted distance has magnitude larger than M_p or prominence larger than P_p .

Selection of M_p and P_p is discussed in Section 4.

3.2.2. Deep vehicle counting

A convolutional NN [12] is used for counting. The model operates on the raw predicted distance and estimates the vehicle count directly, without an intermediate local minima detection. It consists of 1D convolutional, a global-average pooling and fully-connected layers. The global-average-pooling allows the model to operate on varying length distance [13].

The model is trained to predict the vehicle count directly. We experimented with three different loss functions: L_1 , L_2 and smooth L_0 distances. The model trained with smooth L_0 distance gives the best performance. Training with smooth L_0 is performed using a surrogate learned via a deep embedding, where the Euclidean distance between the prediction and the ground truth corresponds to the L_0 distance [14]. The deep embedding is realized using a shallow FCNN. The surrogate and the counting model are trained in parallel.

3.3. Implementation details

The HF-LMS feature is based on the spectrogram of input signal. In this paper, the length of sliding (Hamming) window used in the spectrogram calculation is $N_w = 4096$ and

²The prominence of a peak measures how much the peak stands out due to its height and location relative to other peaks, and is defined as the vertical distance between the peak and its lowest contour line [11].

the stride length is $N_h = 1634$ samples [15], which with 20-second audio files sampled at $f_s = 44100$ Hz gives the time-length of all features of 540 samples. In addition, $N_{mel} = 48$ mel bands are used in HF-LMS, with the lowest frequency $f_{min} = 1000$ Hz ($f_{max} = f_s/2$). To form a vector of input features, we take the HF-LMS spectra at $Q = 5$ preceding and following instants with a stride of 2. Therefore, the dimensionality of the input space is $M = (2Q+1)N_{mel} = 528$. The input dimensionality of Stage 2 FCNN is $2K + 1 = 31$. For distance threshold, we take $T_d = 0.75$ s [8].

Stage 1 and 2 FCNNs have four layers with 528-64-64-1 and 31-31-15-1 neurons per layer, respectively. These configurations gave the best regression performance cross-validated on the training data. Both FCNNs use mean squared error loss, ReLU activation, L_2 kernel regularization with factors 10^{-4} (Stage 1) and 5×10^{-6} (Stage 2), 100 training epochs. Batch normalization is applied at each layer, except for the output, after activation. The model is implemented in Keras. Peak detection is based on `scipy.signal.find_peaks` procedure (SciPy library for Python).

4. EXPERIMENTS

First evaluation metric we will use is *normalized area under the curve* (NAUC) of p_{TP} (T_{det}), i.e., the average value of p_{TP} over the entire detection threshold T_{det} interval [8]. p_{TP} is calculated (as percentage of detected minima within the pass-by intervals, maximum one minimum per interval) at 100 equidistant T_{det} points. The second metric is *relative vehicle counting error*

$$RVCE = (N_v^{true} - N_v^{est}) / N_v^{true} \times 100 [\%], \quad (3)$$

where N_v^{true} and N_v^{est} represent the true and the estimated vehicle count. As opposed to (3), the RVCE definition in [8] uses the absolute difference. Here, the signed RVCE enables distinguishing between counting underestimation (positive RVCE) and overestimation (negative RVCE).

We will use the dataset from [8] which contains two parts: VC-PRG-1:5 (250 20-second audio files with 841 vehicles) and VC-PRG-6 (172 audio files with 580 vehicles). The proposed vehicle counting method (referred to as FCNN-VC) will be trained and validated (80%-20% training-validation split) using VC-PRG-1:5 and tested on VC-PRG-6. We run the method 40 times (training data shuffled each time). Along with the output of Stage 2, we also consider the output of Stage 1 FCNN (denoted as FCNN_{S1}).

Minima detection, and therefore probabilities p_{TP} , p_{FP} and p_{FN} , as well as RVCE, are affected by i) low-pass filtering of the predicted distance, ii) value of M_p and iii) value of P_p (Section 3.2.1). To ensure a fair comparison of performances, we determine an optimal set of parameters for every FCNN-based approach and report only the corresponding optimal results. The optimality criterion is averaged absolute RVCE for detection threshold range $[50\% T_d, T_d]$. We consider all

possible combinations of i) low-pass filters (successive moving average filters (MAFs) with lengths (5, 3)³, (7, 3) and (7, 5, 3)), ii) $M_p \in \{35\% T_d, 40\% T_d, 45\% T_d, 50\% T_d\}$ and iii) $P_p \in \{10\% T_d, 15\% T_d, 20\% T_d, 25\% T_d\}$. The optimal parameters for FCNN_{S1}-VC and FCNN-VC are presented in the first two rows of Table 1.

Table 1. Optimal minima (vehicle) detection parameters

Setup	Optimal parameters
FCNN _{S1} -VC	MAFs (7, 3), $M_p = 45\% T_d$, $P_p = 25\% T_d$
FCNN-VC	MAFs (5, 3), $M_p = 40\% T_d$, $P_p = 20\% T_d$
FCNN _{f0} -VC	MAFs (5, 3), $M_p = 45\% T_d$, $P_p = 20\% T_d$

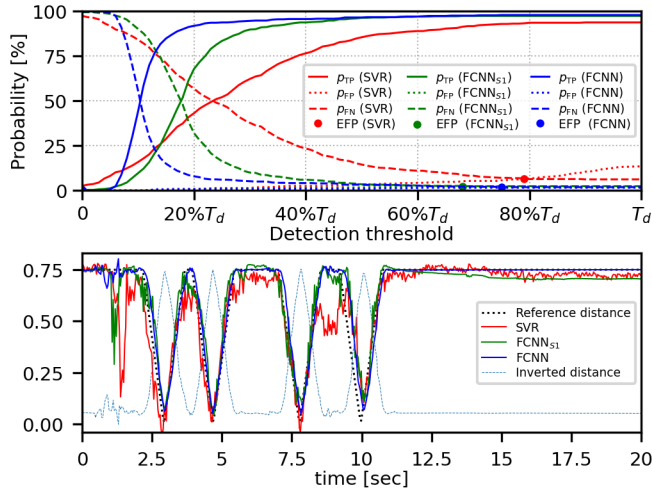


Fig. 3. Top: TP, FP and FN probabilities (see text below). Bottom: Distance predictions of an audio file. Minima are detected by detecting peaks of the inverted predicted distance (blue dashed line).

Figure 3 (top) compares p_{TP} , p_{FP} and p_{FN} of the SVR-based counting [8] (carried out with HFP+LMS) and of one run of FCNN_{S1}-VC and FCNN-VC. Significant improvement is reflected in an increase of NAUC from 0.695 (SVR-VC) to 0.759 (FCNN_{S1}-VC) and 0.850 (FCNN-VC), the latter two averaged over all runs. Dots in Fig. 3 (top) represent the points of equal false probabilities (EFP) [8], which are 6.55% (SVR-VC), 2.33% (FCNN_{S1}-VC) and 1.72% (FCNN-VC).

Figure 3 (bottom) compares distance predictions of one audio file carried out via SVR-VC, FCNN_{S1}-VC and FCNN-VC. The corresponding mean square regression errors for the testing set are 9.55×10^{-3} , 5.27×10^{-3} and 2.30×10^{-3} . The proposed method significantly outperforms SVR-VC in terms of regression accuracy. In addition, Stage 2 improves the regression accuracy with respect to Stage 1.

RVCE plots for detection threshold range $[30\% T_d, T_d]$ are given in Fig. 4 (top). With the exception of SVR, RVCEs are

³ (l_1, l_2) denotes filtering first with an MAF of length l_1 then with an MAF of length l_2 .

shown as 95% confidence intervals for the mean (CIM). In addition to SVR-VC, FCNN_{S1}-VC and FCNN-VC, we present RVCE of the deep counting approach (Section 3.2.2) and of FCNN-VC when full-frequency range is used in LMS input features ($f_{min} = 0$, see Section 3.3). The latter is denoted as FCNN_{f0}-VC and its optimal parameters are given in the bottom row in Table 1. CIM of Deep-VC RVCE is a horizontal band within $[1.25\%, 2.49\%]$. FCNN-VC outperforms the other approaches by a significant margin. Its 95% CIM goes below 2% for detection threshold around 50% T_d and is within $[0.28\%, -0.55\%]$ for thresholds above 70% T_d .

The combined peak magnitude-prominence criterion in minima detection (Section 3.2.1) improves the counting performance with respect to detection based solely on the peak prominence [8], as illustrated in Fig. 4 (bottom). Peak prominences of 5%, 10% and 15% are considered, after applying two successive MAFs with lengths 5 and 3.

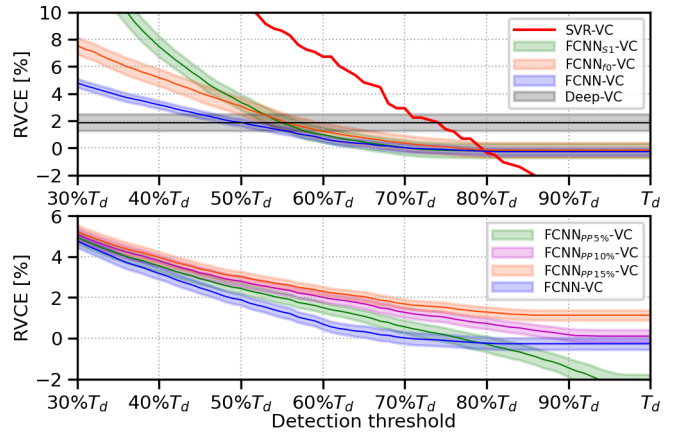


Fig. 4. Relative vehicle counting error, RVCE, as a function of the detection threshold. With the exception of SVR, RVCEs are shown as 95% confidence intervals for the mean. The proposed FCNN-VC (in blue) compared with alternatives (for their description, see text).

5. CONCLUSIONS

We proposed a method for acoustic vehicle counting based on the clipped vehicle-to-microphone distance. The distance was predicted using a two-stage NN-based regression. Significant improvement in regression accuracy with respect to the SVR-based approach resulted in a highly accurate vehicle counting not depending on detection threshold within a wide range of threshold values. Deep counting, an alternative to the local minima-based counting, estimates the vehicle count directly from the predicted distance, without detecting local minima. Although outperformed in accuracy by the latter approach, a significant advantage of deep counting is that it does not depend on minima detection parameters. Our future work will address developing end-to-end vehicle counting method.

6. REFERENCES

- [1] Myounggyu Won, “Intelligent traffic monitoring systems for vehicle classification: A survey,” *IEEE Access*, vol. 8, pp. 73340–73358, 2020.
- [2] Milind Naphade et al., “The 2019 AI City challenge,” in *CVPR Workshops*, 2019, pp. 452–460.
- [3] Brendan Tran Morris and Mohan Manubhai Trivedi, “A survey of vision-based trajectory learning and analysis for surveillance,” *IEEE Transactions on Circuits and Systems for Video Technology*, vol. 18, no. 8, pp. 1114–1127, 2008.
- [4] Jien Kato, “An attempt to acquire traffic density by using road traffic sound,” in *Proceedings of the 2005 International Conference on Active Media Technology, 2005.(AMT 2005)*. IEEE, 2005, pp. 353–358.
- [5] Jobin George, Leena Mary, and KS Riyas, “Vehicle detection and classification from acoustic signal using ANN and KNN,” in *2013 international conference on control communication and computing (ICCC)*. IEEE, 2013, pp. 436–439.
- [6] Jobin George, Anila Cyril, Bino I Koshy, and Leena Mary, “Exploring sound signature for vehicle detection and classification using ANN,” *International Journal on Soft Computing*, vol. 4, no. 2, pp. 29, 2013.
- [7] Sugang Li, Xiaoran Fan, Yanyong Zhang, Wade Trappe, Janne Lindqvist, and Richard E Howard, “Auto++: Detecting cars using embedded microphones in real-time,” *Proceedings of the ACM on Interactive, Mobile, Wearable and Ubiquitous Technologies*, vol. 1, no. 3, pp. 70, 2017.
- [8] Slobodan Djukanović, Jiří Matas, and Tuomas Virtanen, “Robust audio-based vehicle counting in low-to-moderate traffic flow,” in *2020 IEEE Intelligent Vehicles Symposium (IV)*, 2020.
- [9] Chih-Chung Chang and Chih-Jen Lin, “LIBSVM: A library for support vector machines,” *ACM Transactions on Intelligent Systems and Technology (TIST)*, vol. 2, no. 3, pp. 1–27, 2011.
- [10] Romain Serizel, Victor Bisot, Slim Essid, and Gaël Richard, “Acoustic features for environmental sound analysis,” in *Computational Analysis of Sound Scenes and Events*, pp. 71–101. Springer, 2018.
- [11] “Topographic prominence,” https://en.wikipedia.org/wiki/Topographic_prominence, Accessed: 2020-10-19.
- [12] Xiang Zhang, Junbo Zhao, and Yann LeCun, “Character-level convolutional networks for text classification,” in *NeurIPS*, 2015.
- [13] Min Lin, Qiang Chen, and Shuicheng Yan, “Network in network,” *ICLR*, 2014.
- [14] Yash Patel, Tomas Hodan, and Jiri Matas, “Learning surrogates via deep embedding,” *ECCV*, 2020.
- [15] Ljubiša Stanković, Igor Djurović, Srdjan Stanković, Marko Simeunović, Slobodan Djukanović, and Miloš Daković, “Instantaneous frequency in time–frequency analysis: Enhanced concepts and performance of estimation algorithms,” *Digital Signal Processing*, vol. 35, pp. 1–13, 2014.